PROCEEDINGS, 46th Workshop on Geothermal Reservoir Engineering
Stanford University, Stanford, California, February 15-17, 2021
SGP-TR-218

Coupling subsurface and above-surface models for optimizing the design of borefields and district heating and cooling systems in the presence of varying water-table depth

Christine Doughty, Jianjun Hu, Patrick Dobson, Peter Nico, Michael Wetter

Lawrence Berkeley National Laboratory, Berkeley, CA, USA

{jianjunhu, cadoughty, pfdobson, psnico, mwetter}@lbl.gov

Keywords: Modelica Buildings Library, TOUGH, Borefields, Reservoir, District heating and cooling, Code coupling

ABSTRACT

Dynamic energy simulation is important for the design and sizing of district heating and cooling systems with geothermal heat exchange. Current modeling approaches in building and district energy simulation tools typically consider heat conduction through the ground between boreholes, without flow of groundwater. On the other hand, detailed simulation tools for subsurface heat and mass transfer exist, but these fall short in simulating above-surface energy systems.

To support the design and operation of such systems, we have developed a coupled model including a software package for building and district energy simulation, and software for detailed heat and mass transfer in the ground. For the first, we use the open-source Modelica Buildings Library, which includes dynamic simulation models for building and district energy and control systems. For the heat and mass transfer in the soil, we use the TOUGH simulator. TOUGH can model heat and multi-phase, multi-component mass transport for a variety of fluid systems, as well as chemical reactions, in fractured porous media.

In previous work, we described the coupling of these software packages, including how time-dependent boundary conditions for the borehole walls are synchronized for use in Modelica and TOUGH. We verified that the coupled Modelica/TOUGH code produced consistent results with the original Modelica code for an idealized problem in which heat transfer was purely by conduction in a uniform geologic medium. Here, we examine less idealized problems for which TOUGH's advanced capabilities for modeling fluid flow are required. The first problem has a shallow vadose zone, and the second problem has a thicker vadose zone with a water-table depth that varies in time, which requires a fine vertical grid discretization for the TOUGH model.

1. INTRODUCTION

Geothermal resources are considered a clean and sustainable form of renewable energy and have been applied as the heating and cooling source and for thermal energy storage in district heating and cooling (DHC) systems. Simulation and optimization of DHC systems requires efficient and reliable models of the individual elements in order to correctly represent heat losses and gains, temperature propagation and pressure drops. When a geothermal borefield is present in the loop of the DHC system, the usual approach is to consider heat transfer in the subsurface to be purely by thermal conduction between the pipes and the surrounding soil and rock, with no consideration of fluid flow in the soil and rock. Coupling the DHC system to a subsurface model that can consider coupled fluid and heat flow loads in the soil and rock is still a challenge, which we address here through the coupling of the Modelica Buildings Library and subsurface flow and transport simulator TOUGH.

The open-source Modelica Buildings Library (Wetter et al., 2014) developed by Lawrence Berkeley National Laboratory (LBNL), which includes dynamic simulation models for building and district energy and control systems, has models for closed-loop borefields (Picard and Helsen, 2014), based on so-called g-functions (Claesson and Javed, 2012). The models solve the transient heat flux in the ground by discretizing the ground surrounding the borehole in several cylindrical layers. The layer temperature at this outer radius is calculated using an approximation of the line-source theory together with superposition. However, this model assumes that heat transfer in the ground is purely by conduction, with no groundwater flow. TOUGH3 (Jung et al., 2018), the successor to TOUGH2 (Pruess et al., 2012), which was also developed by LBNL, simulates fluid flow and heat transport in heterogeneous geologic settings, including fractured rock, at scales ranging from core-scale to basin-scale. TOUGH considers multi-phase, multi-component fluid and heat flow in porous and fractured media. It employs the integral finite difference method for spatial discretization, enabling efficient, realistic representation of complex geologic and hydrologic features including grid layers that conform to tilted or warped beds, stochastic property assignments to represent highly heterogeneous formations, and local grid refinement. TOUGH incorporates accurate phase-partitioning and thermophysical properties of all fluid phases and components. Various equation of state packages are available to represent different fluid combinations, such as the package EOS3, which considers components water and air, in liquid and gaseous phases, and is the relevant equation of state for aquifer or borehole thermal energy storage. The related code TOUGHREACT (Xu et al., 2014) adds the capability of including geochemical reactions, which may be added to the Modelica coupling in the future.

The key processes that TOUGH considers that are not included in the stand-alone Modelica treatment of the subsurface using g-functions may be divided into saturated-zone processes and vadose-zone processes. In the saturated zone beneath the water table, thermal conductivity and heat capacity may vary with local geology, and convective heat flow accompanies groundwater flow, which could be buoyancy flow arising from the injection of warm or cold water, or regional groundwater flow. In the vadose zone, thermal conductivity and heat capacity of rock with air-filled pore spaces are much smaller than those with water-filled pore spaces, and gas-phase flow

involving water vapor and air may occur, greatly impacting surface heat transfer. Baser et al. (2018) and Moradi et al. (2016) have noted the importance of gas flow in the vadose zone for borehole energy storage systems. Additionally, thermal properties would vary temporally with a changing water table, and latent heat effects accompanying evaporation or condensation could be significant for high-temperature systems.

In a previous paper (Hu et al., 2020), we presented a modeling approach to couple the above-surface DHC system modeling with Modelica and subsurface ground response modeling with TOUGH. We described the coupling approach and then validated it by applying the coupled model to the idealized case representing one borehole as a symmetry element within a large borefield, with uniform thermal conductivity and no fluid flow in the subsurface. We found that the coupled Modelica/TOUGH model produced results that agreed well with the original Modelica model incorporating g-functions. In the present paper, we describe a series of cases with an axisymmetric geometry, as in previous studies, but with a vadose zone overlying a saturated zone, in which significant groundwater flow may occur by virtue of a seasonally variable water table.

2. BOREHOLE AND BOREFIELD GEOMETRY

As in the previous study (Hu et al., 2020), we consider a DHC system with three building types (office, hospital, and apartment) and a sewage heat-exchange station, which includes a single-U-tube borefield as its cooling and heating source. We assumed that the borefield has following characteristics, illustrated in Figure 1 with parameters given in Table 1:

- Boreholes are connected in parallel.
- Boreholes are uniformly distributed and the distances *DBor* between them are the same.
- All boreholes have the same inlet water flow rate and temperature.
- All boreholes have the same length *hBor*, the same radius *rBor*, and are buried at the same depth *dBor* below the ground surface.
- The conductivity, capacitance and density of the grout and pipe material are constant, homogeneous and isotropic.
- Inside the borehole, the non-advective heat transfer is only in the radial direction.
- The borehole length is divided into multiple segments (*N*) and each segment has a uniform temperature.
- Initial ground temperature has a profile as shown in Figure 1c.

Based on these assumptions, all boreholes within the borefield behave identically, so only one need be modeled. Within Modelica, the borehole is discretized along the depth *z*. Within each segment, the temperatures of the cool downward-flowing leg of the U-tube and the warm upward-flowing leg of the U-tube are modeled with circuit theory to produce a single temperature $T_b(z, t)$ representative of the borehole temperature for that segment (Figures 1a and 1b). It is $T_b(z, t)$ that is passed to and from TOUGH, along with the heat source/sink strength $Q(z, t)$, which is a function of time that depends on the energy supply and demand of the DHC system. The coupling is described in detail in Hu et al. (2020), but the basic idea is that Modelica calls TOUGH at time t_M for a synchronization time step of duration dt_M, with $T_b(z, t_M)$ and $Q(z, t_M)$ specified. TOUGH then simulates the subsurface fluid and heat flow, using as many time steps dt_T as required to reach dt_M. Typically, $dt_T = dt_M$, but if complex flow processes are occurring, then $dt_T << dt_M$ is possible. TOUGH then returns $T_b(z, t_M+dt_M)$ to Modelica, which uses it for the next Modelica time step.

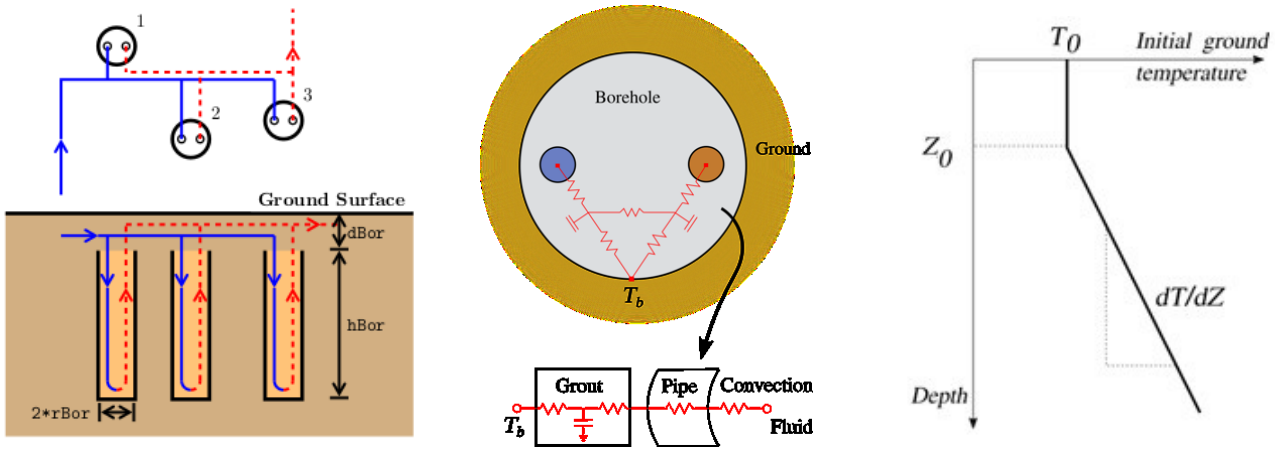

a) b) c)

Figure 1: Assumptions used in this study: a) typical single-U-tube borefield, shown here with heat being extracted from the subsurface; b) thermal network of each borehole segment; c) initial ground temperature

Table 1: Parameters and the values used for the borefield

Parameter	Value	Description
hBor	100 m	Height of the borehole
N	10	Number of borehole segments
rBor	0.075 m	Borehole radius
dBor	1.0 m	Depth of top of borehole
DBor	6.0 m	Distance between boreholes
m_flow	0.02~0.24 kg/s	Water flow rate in the U-tube within the borehole
dT/dZ	0.01 or 0.025 K/m	Vertical temperature gradient of undisturbed soil/rock
T_0	10 or 15°C	Surface temperature
Z_0	10 m	Depth below which temperature gradient starts

3. SHALLOW WATER TABLE CASES

The assumption of uniform thermal conductivity that was employed in previous studies (Hu et al., 2020) is not very good when a vadose zone exists, because thermal properties of dry or partially-saturated soil differ significantly from those of liquid-saturated soil. As a first test case, we assume a water table at 10 m below the ground surface, with a partially saturated vadose zone above it and fully liquid-saturated conditions below, extending to the bottom of the model. The TOUGH grid is the same one used in previous studies, and has 10-m thick layers, corresponding to the Modelica discretization of the borehole. This vertical discretization is really too coarse to properly represent a water table and vadose zone, so these results must be considered preliminary. We consider surface temperature T_0=10°C, and gradient dT/dz = 0.01 K/m. The surface boundary condition must now also describe fluid flow, and we consider the surface to be pure gas phase, at atmospheric pressure, with a relative humidity of 0.5. We run a gravity-capillary pressure equilibration simulation with no borehole heat source/sink to establish the capillary fringe as the initial condition, then do a coupled Modelica/TOUGH simulation in which TOUGH calculates coupled fluid and heat flow. This approach is denoted Case 3 below.

As a simpler alternative to simulating coupled fluid and heat flow with TOUGH, we can take the liquid saturation profile from the capillary fringe, $S_l(z)$, and use it to determine a thermal conductivity profile $\lambda(z)$, using $\lambda(S_l)=\lambda_{dry} + S_l^{1/2}(\lambda_{wet} - \lambda_{dry})$, where λ_{dry} =0.5 W/(m K) and λ_{wet} =2.5 W/(m K). This square-root dependence of λ on S_l is commonly used (e.g., Akrouch et al., 2016), and is the default choice in TOUGH, but other options are possible (Dong et al., 2015). Then this thermal conductivity profile is assigned layer by layer to the TOUGH grid, and a coupled Modelica/TOUGH simulation is run in which TOUGH considers conduction only. This approach is denoted Case 2 below.

Figure 2 compares results for Cases 2 and 3 with results from Hu et al. (2020): conduction only with a uniform thermal conductivity (Case 0) and Modelica with a g-function. All four cases produce essentially the same results for the borehole wall temperature and the heat flow to and from the subsurface. That is, there is no significant effect of the vadose zone on heat flow. Case 3 indicates that fluid flow is minimal, so the only effect possible would be due to the different thermal properties of the vadose zone. But apparently, the vadose zone is so thin (10 m) compared to the entire length of the borehole (100 m) that this effect is insignificant.

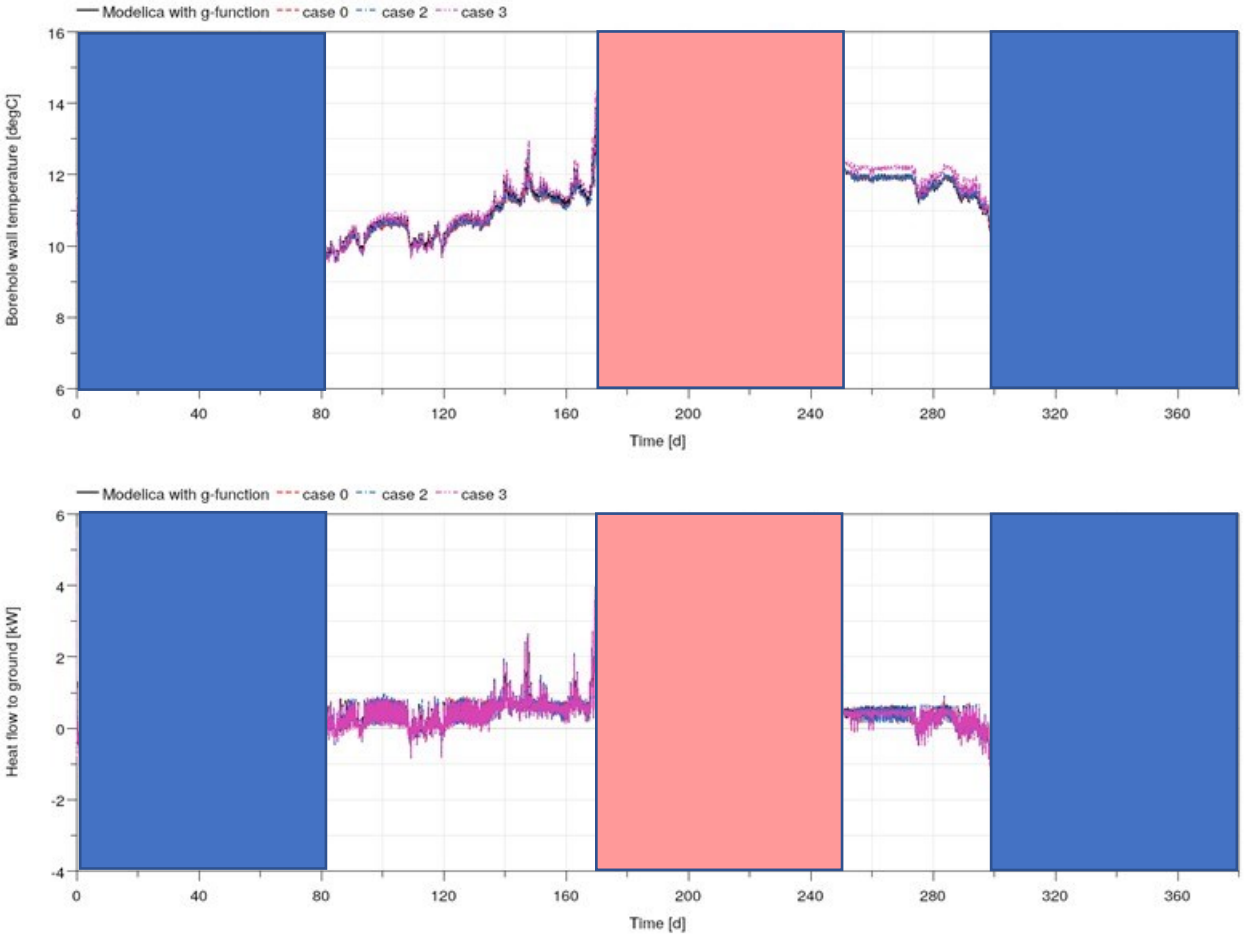

Figure 2: Comparison of the original Modelica with a g-function to coupled Modelica/TOUGH simulations for: conduction only with uniform thermal properties (Case 0), conduction only with layered thermal properties to mimic a vadose zone (Case 2), and coupled fluid and heat flow (Case 3). Top frame: borehole wall temperature (averaged over 100 m long borehole); bottom frame: heat flow into (positive) or out of (negative) the subsurface. Recall that the initial ground temperature varies between 10-11 C, so when borehole wall temperature $T < 10$, heat is being extracted from the ground, and when $T > 11$ heat is being charged into the ground. Shading: cooling season - blue, heating season - red, shoulder seasons - unshaded.

Figure 3 illustrates the results of the coupled Modelica/TOUGH simulations for g-function, Case 0, and Case 3 in more detail, by plotting the temperature at the top and the bottom of the borehole wall over a one-year period. For the g-function, the temperature difference between the top and bottom is constant, and always equal to 1 K, which is the specified initial condition: 10°C at the top of the borehole and 11°C at the bottom. Because the g-function calculates heat transfer for the entire borehole at once, the temperature difference between the top and the bottom that exists at the beginning of the simulation is maintained throughout. This is not a physical effect, but rather is a limitation of using one g-function for the whole depth of the borehole.

For Cases 0 and 3, for cold days when the above-surface energy system is harvesting heat by circulating cold water through the U-tube, the top of the borehole is cooler than the bottom as cool water flows into the subsurface and is heated up. For hot days, the reverse occurs, with hot water being injected and cooling off as it transfers heat to the ground. The temperature difference for Case 3 is bigger than that for Case 0. Close examination of Figure 3 reveals that T_{top} is more extreme for Case 3 (colder on cold days when cold water is being injected and hotter on hot days when hot water is being injected), whereas T_{bot} is the same for both cases. This difference in T_{top} occurs because the thermal conductivity for Case 3 is much lower than that for Case 0 (dry soil versus saturated soil), so heat does not spread out in the soil as much, leaving more extreme temperature at the borehole. For this shallow vadose zone, most of borehole length is saturated, so most of system is the same for Cases 0 and 3, thus the average borehole temperature (Figure 2) agrees between all cases.

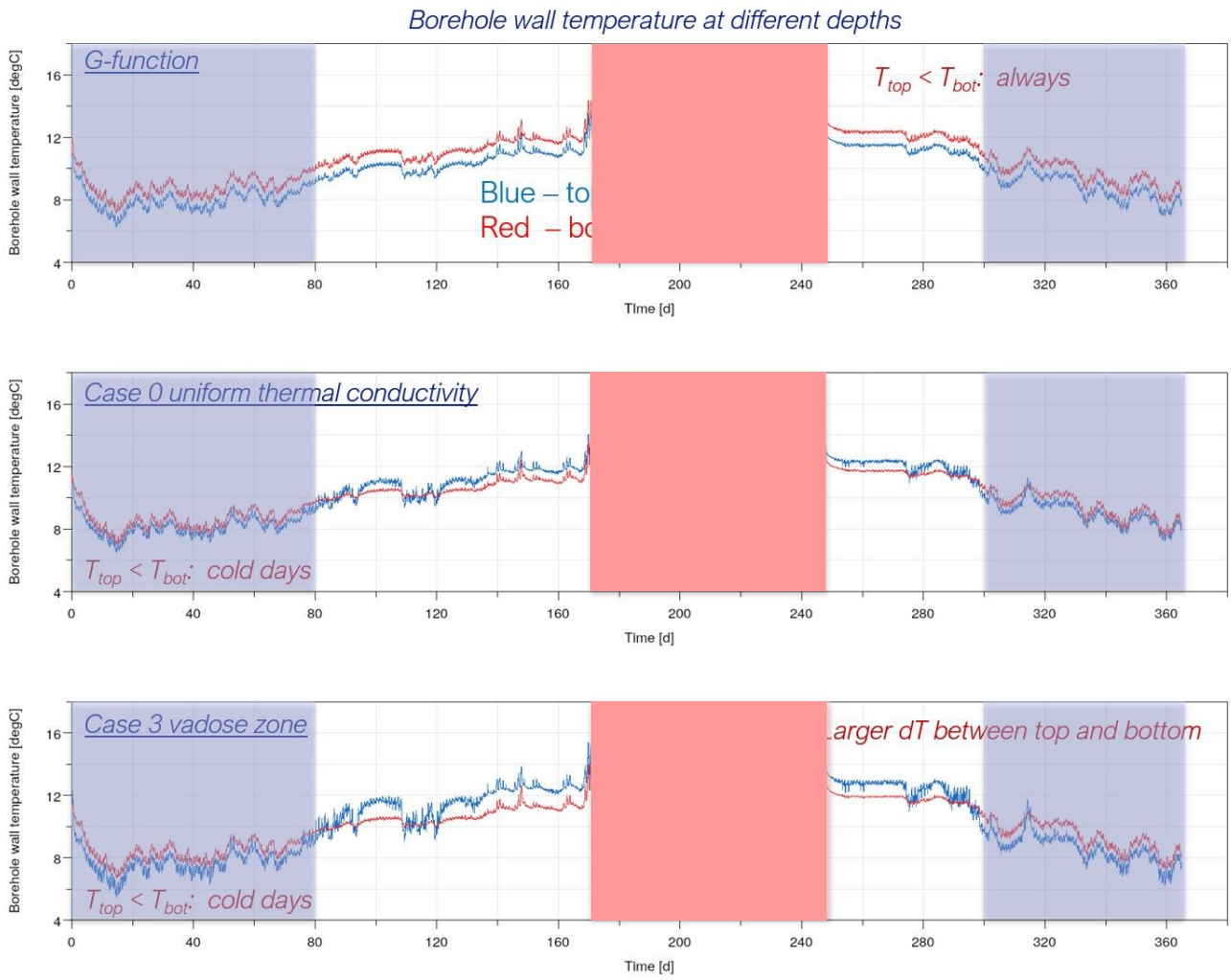

Figure 3: Comparison of the original Modelica with a g-function to coupled Modelica/TOUGH simulations for: conduction only with uniform thermal properties (Case 0) and coupled fluid and heat flow (Case 3). Each frame shows the temperature at the top (blue) and bottom (red) of the borehole. Shading: cooling season - blue, heating season - red, shoulder seasons - unshaded.

4. DEEP WATER TABLE CASES

Because the preliminary studies with a shallow water table described in the previous section showed that a thin vadose zone above a shallow water table had little impact on heat flow, we developed a model with a much deeper water table, at a depth of 51 m, so that only half the borehole length of 100 m would be in the saturated zone. Below, we describe this model and illustrate stand-alone TOUGH simulations. This model will be coupled with Modelica in future work.

4.1 Grid

The axisymmetric grid for the TOUGH model is shown in Figure 4. Note that the radial scale is greatly exaggerated compared to the vertical scale. The grid contains 42 layers altogether, of which 33 are used to represent the borehole (layers 4-36). Grid layer thickness above the water table ranges from 0.5 m to 5 m, to adequately resolve changes in the vadose zone. Near the water table itself, layer thickness is 1 m, because experience running TOUGH for vadose-zone problems has shown that fine grids are necessary when water-table depth can change, resulting in phase transitions between single-phase liquid and two-phase liquid-gas conditions for grid blocks at the water table. Thinner layers are also used near the surface and at the bottom of the borehole, to resolve sharper temperature gradients anticipated at these locations. Radially, the grid is composed of 30 columns, with finer discretization close to the borehole. The innermost column has the same radial dimension as the borehole itself, 0.075 m.

Unlike the grid used for previous studies in which TOUGH is coupled to Modelica, here there is not a one-to-one correspondence between Modelica grid blocks (10 blocks, each being 10 m thick) and TOUGH grid blocks (33 grid blocks with variable thickness ranging from 1 m to 10 m). Hence, each call to TOUGH, at the start of the time step, the temperature at each Modelica grid block will be assigned to one or more TOUGH grid blocks, and at the end of the time step, the temperature at each TOUGH grid block will be averaged with its

neighbors to provide a temperature for the corresponding Modelica grid block. The TOUGH grid block thicknesses are designed so that groups of adjacent grid blocks have a thickness equal to the Modelica 10-m thickness (i.e, 2 x 5 m, 10 x 1 m, 5 + 2.5 + 1.5 + 1, etc). For groups of TOUGH grid blocks with different thicknesses, the temperature will be a weighted average based on grid-block thickness.

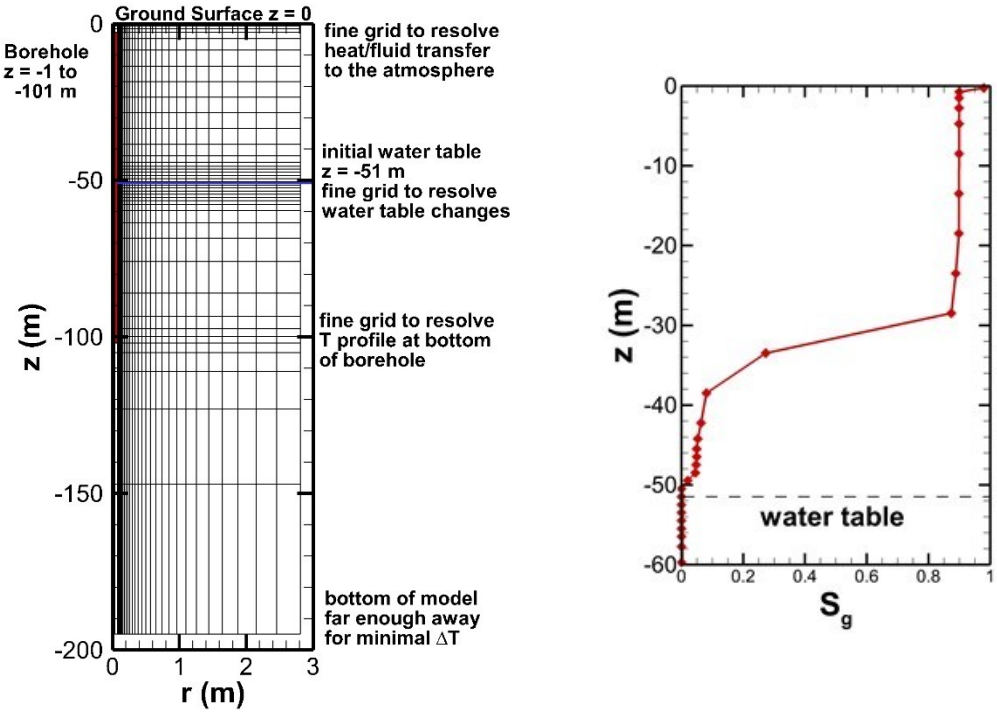

Figure 4: TOUGH grid used for deep water table cases and the initial condition for gas saturation, showing the capillary fringe above the water table.

4.2 Initial and Boundary Conditions

The geothermal gradient used previously as the temperature initial condition (T_0 = 10°C, dT/dz = 0.01 K/m) has been altered to be more consistent with a thick vadose zone: T_0 = 15°C, dT/dz = 0.025 C/m. As before, the initial temperature is constant for the uppermost 10 m of the subsurface.

Prior to modeling the borehole heat transfer problem, a preliminary simulation is necessary to establish the capillary fringe**.** First a saturation distribution with no water above the water table at 51 m depth, and full saturation below the water table is specified. Then the model is run isothermally with relative humidity of 1 at the surface for a few hundred years. This capillary/gravity equilibration produces a capillary fringe above the water table (Figure 4), and a hydrostatic pressure profile below it. For the main simulation, relative humidity at the surface is set to 0.5. Other surface boundary conditions are pure gas phase, constant pressure at 1 atm, and the sinusoidal temperature variation shown in Figure 5, with mean (16°C) and amplitude (6 K) determined by fitting to a one-year temperature record for Walnut Creek, CA (NOAA, 2021).

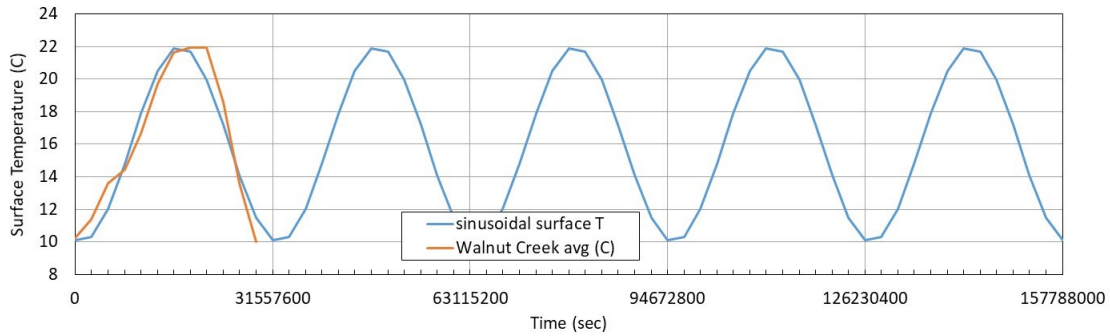

Figure 5: Temperature boundary condition assigned at the surface of the TOUGH model (blue), and the one-year temperature record on which it is based (orange).

The borehole heat source/sink, shown in Figure 6, is seasonal, and is in phase with the surface temperature, having a minimum at $t = 0$, which corresponds to January 1. This heat source is meant to roughly mimic the nature of the heat source/sink provided by the water that flows in the pipes of the borefield.

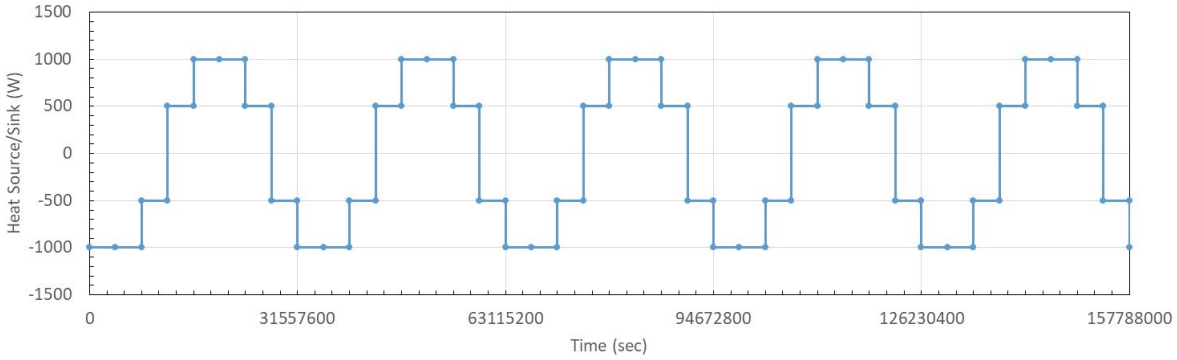

Figure 6: Heat source (positive)/sink (negative) applied to borehole in TOUGH model.

Some of the cases considered have a variable depth water table. This is achieved by specifying a sinusoidally varying pressure at the bottom boundary of the model, as shown in Figure 7. The mean and amplitude of the pressure variation are chosen by trial and error in order to achieve about a 10 m variation in the depth of the top of the capillary fringe. The minimum pressure is set to occur on October 1 (23,668,200 sec in Figure 7), which historically represents the beginning of the rainy season in Northern California, when the water table and capillary fringe are expected to be deepest.

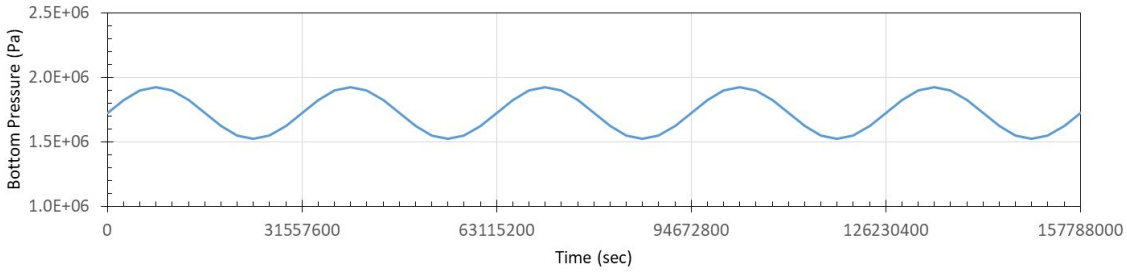

Figure 7: Pressure boundary condition assigned at the bottom boundary of the TOUGH model.

4.3 Four Cases

Four cases are chosen to be simulated with TOUGH, to create a variety of fluid flow conditions. We consider both constant and variable water tables, and low (1E-13 m^2 = 100 mD) and high (1E-11 m^2 = 10 D) permeabilities (Table 2). We use van Genuchten (1980) relative permeability and capillary pressure curves, with Leverett scaling for capillary pressure, meaning the capillary fringe has different $S_l(z)$ profiles for low and high permeability cases. The two permeability values were chosen to provide saturated-zone Rayleigh numbers above and below the critical Rayleigh Number, so that natural convection is not expected for the low-permeability case, but is for the high permeability case. The low permeability is the same value used in the shallow water table studies, where minimal fluid flow was observed.

Table 2: For cases for stand-alone TOUGH simulations

		Bottom Pressure	
		Constant	Sinusoidal
Permeability	low	j01c	j01
	high	j02c	j02

4.4 TOUGH Stand-Alone Results

Figure 8 shows snapshots of gas saturation and temperature for case J02c, which has a constant water table and high permeability. The water table is at z = -51 m, with the capillary fringe showing increasing gas content at shallower depths. The temperature close to the borehole is higher during the heat-charging period (left two frames) and lower during the heat-discharging period (right two frames) in the upper portion of the vadose zone, where gas content is higher, due to the lower thermal conductivity of dry soil. During the heat-charging period, a clockwise convection cell develops beneath the water table and in the wetter portion of the capillary fringe (below -30 m), which reverses direction during the heat-discharging period. No such convection occurs for the low permeability case J01c, consistent with its saturated-zone Rayleigh number being smaller than the critical value. Gas-phase flow occurs in the drier shallow portion of the vadose zone, and is mainly out and in from the borehole rather than forming a convection cell. For gas-phase flow in the vadose zone, several authors have proposed vadose-zone Rayleigh numbers (Catoloco et al., 2016; Amili and Yortsos, 2004), but their formulations give values that differ by several orders of magnitude, making their use difficult to justify. Nonetheless, even the high-permeability case provides vadose-zone Rayleigh numbers much smaller than the critical value using either formulation. This is consistent with the gas flow pattern seen in Figure 8.

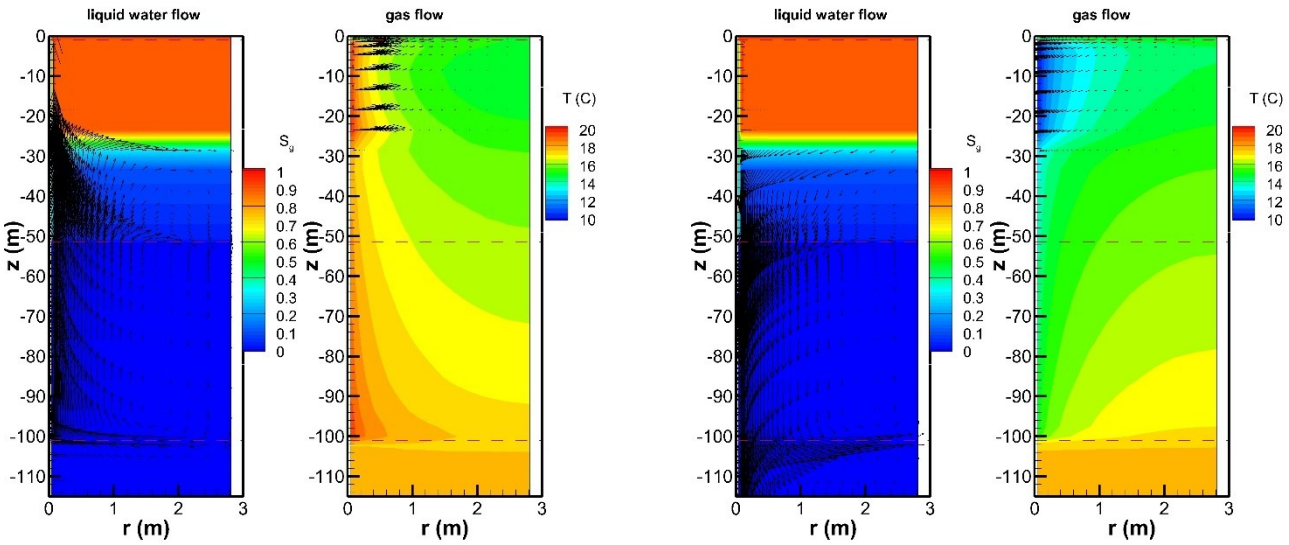

Figure 8: Snapshots of gas saturation, temperature, liquid flow and gas flow for case J02C (constant water table, high permeability). Left two frames: during heat-charging period, right two frames: during heat-discharging period. The red dashed lines show the top and bottom of the borehole at depths of 1 and 101 m, and the water table at a depth of 51 m.

Figure 9 shows the same images for case J02, which has a variable water table and high permeability. Both liquid and gas fluid flows show large upward and downward flow. The vector length scale is the same for all gas-flow images, but it is 10 times smaller for the liquid-flow images for the variable water table case, meaning these up and down flows are much larger than the natural convection cell flow shown in Figure 8. Despite the strongly different flow fields, the temperature distributions are nearly the same for the two cases, indicating that heat flow is conduction dominated.

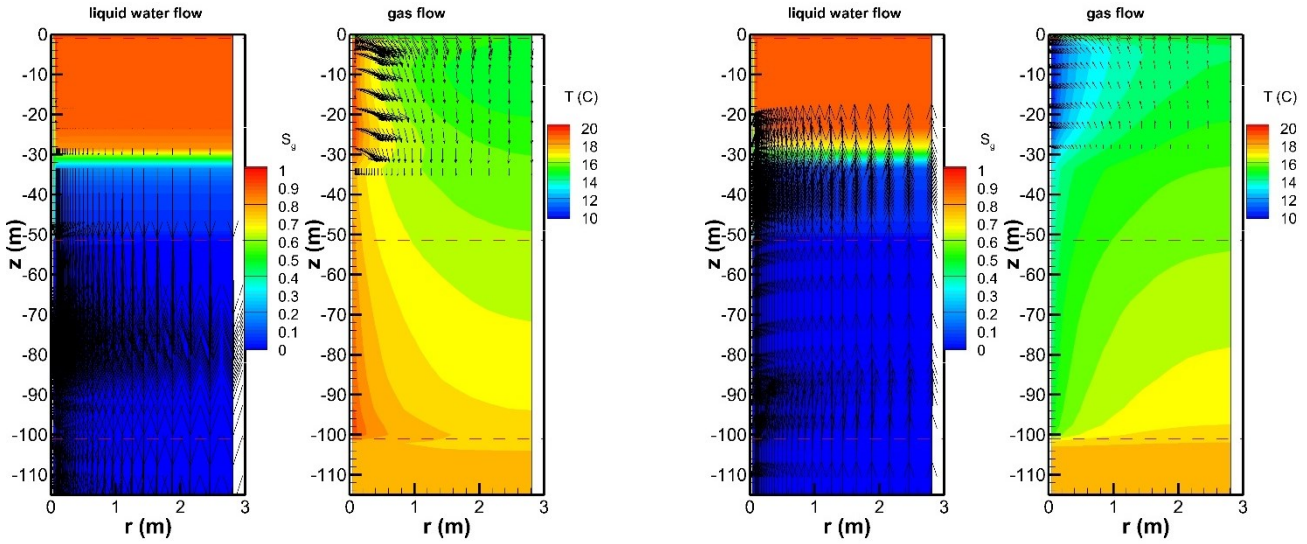

Figure 9: Snapshots of gas saturation, temperature, liquid flow and gas flow for case J02 (variable water table, high permeability). Left two frames: during heat-charging period, right two frames: during heat-discharging period. The red dashed lines show the top and bottom of the borehole at depths of 1 and 101 m, and the water table at a depth of 51 m. Reference length for liquid flow vectors is 10 times smaller than in Figure 8.

Figure 10 shows the gas saturation distributions at a series of times for case J02, illustrating how the water table and capillary fringe vary over the course of one year. Although the depth of the water table itself (black contour line) only varies by about 1 m, the thickness and depth of the capillary fringe vary by much more, almost 10 m. Additionally, the saturation distribution within the capillary fringe changes over time.

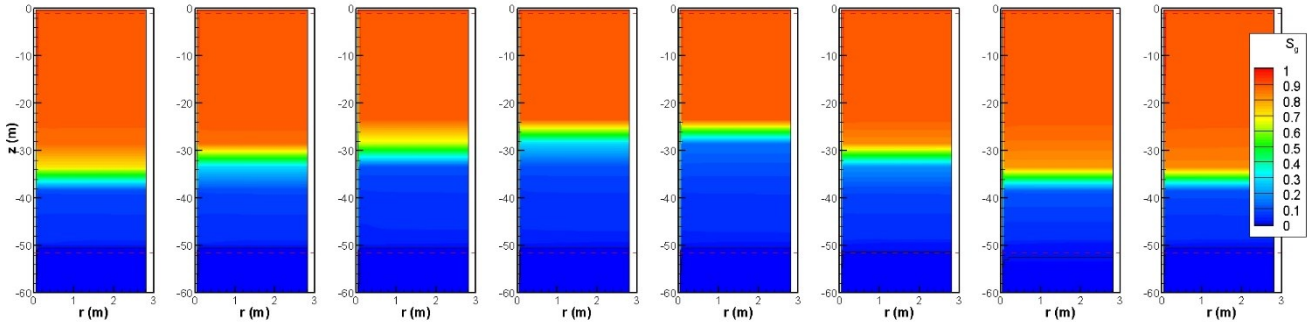

Figure 10: Snapshots of gas saturation for case J02 (variable water table, high permeability) every 1.5 months over a one-year period, illustrating the motion of the water table and capillary fringe. The black contour line shows $S_g = 0$.

Figure 11 shows advective gas-phase flow in and out through the ground surface. Liquid water is also present in the vadose zone, but at the surface it is either absent or immobile, so the only fluid phase entering or leaving the subsurface is the gas phase. The gas phase is mainly composed of air, with only a small amount of water vapor, so the plot essentially shows the advective flow of air. Gas also flows by binary diffusion, with a balanced counterflow of water vapor and air. It turns out that the diffusive and advective flows of air nearly cancel out, so the plot is a good representation of diffusive water-vapor flow.

For the constant water-table cases (J01c and J02c), water-vapor flow is always out of the subsurface, producing a gradual drying of the vadose zone. At about four years (t=126230400 sec), the top of the capillary fringe drops one grid block, which produces a sharp decrease in gas flow. The sharpness is a numerical artifact, but the decrease of water-vapor flow out of the subsurface with drying of the vadose zone is physical. The decrease occurs earlier for the high-permeability case J02c than for the low-permeability case J01C, which is reasonable given the weaker capillary pressure for that case.

For the variable water-table cases (J01 and J02), gas flow out of the subsurface decreases when the water table is declining, and even reverses direction, especially for the high-permeability case J02. The water table variation just has one maximum and minimum per year, following the imposed pressure variation shown in Figure 7, but the vadose zone is highly compressible, and the two-phase flow is strongly non-linear, so that variation of the top of the capillary fringe has multiple peaks during both periods of increasing and declining water table level (Figure 10), which is reflected in the surface gas flow.

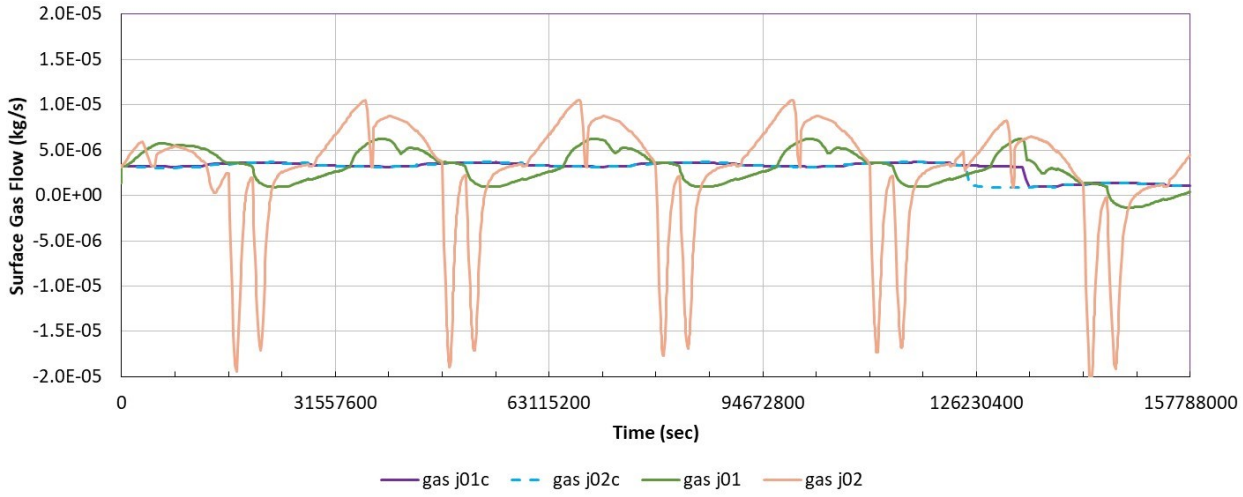

Figure 11: Surface advective gas-phase flow for the four cases. Positive values represent flow out of the subsurface.

Figure 12 shows the heat flow through the ground surface for the four cases. The four curves are indistinguishable, despite the large variability in gas flow through the surface shown in Figure 10, implying that heat flow out of the surface is dominated by conduction. The surface heat flow is closely correlated with the imposed heat source/sink at the borehole, but with a slight phase lag, due to the delay in heat transfer from the borehole to the ground surface. Note that the surface heat flow is just a small fraction of the imposed heat source/sink, which makes sense considering the extreme aspect ratio of the storage volume: over 100 m deep but only 3 m in radial extent.

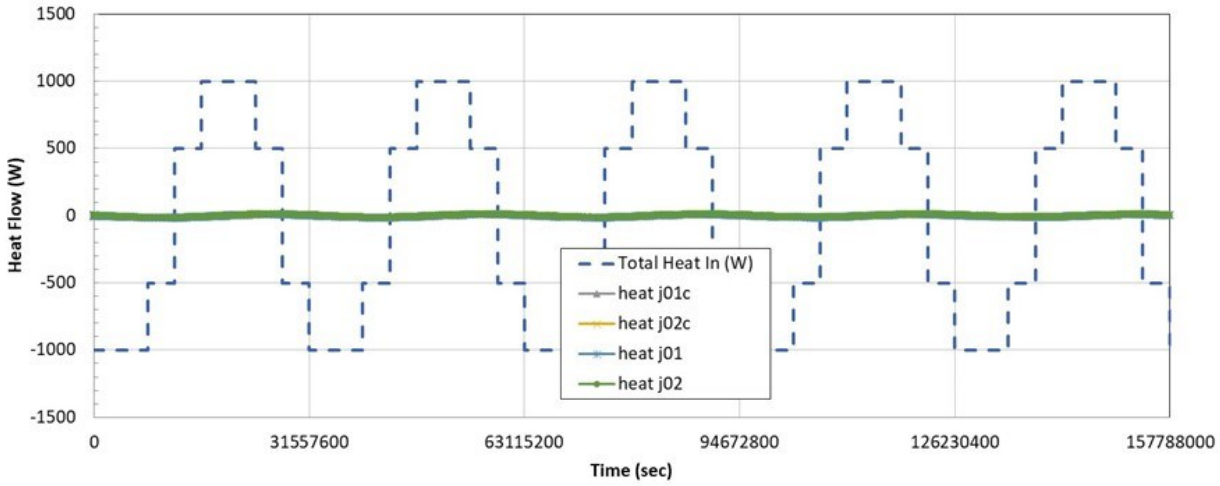

Figure 12: Surface heat flow for the four cases, with positive values representing heat flow out of the subsurface. The curves for all four cases overlie one another. The imposed heat source/sink at the borehole is also shown.

Figure 13 shows the temperature at the top of the borehole (z = -1 m). All four cases show very similar responses, which are closely correlated to the imposed heat source/sink at the borehole. Hence, despite the large differences in fluid flow inside the soil for the different cases, the boundary temperature $T_b(-1, t)$ of the system is about the same for all cases.

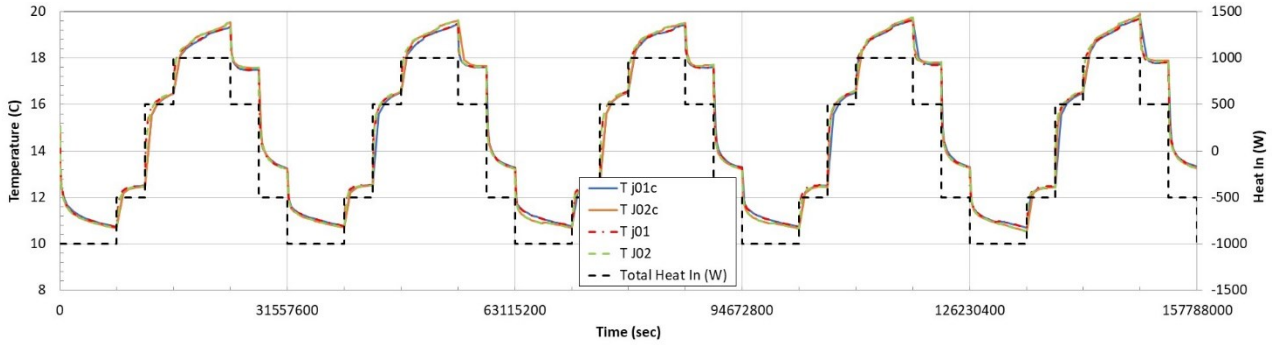

Figure 13: Temperature at the top of the borehole for the four cases. The dashed line shows the imposed heat source/sink at the borehole.

5. CONCLUSIONS

We continue to develop the coupling between Modelica and TOUGH, by considering less ideal cases than in previous studies (Hu et al., 2020). We first considered a shallow water table with a thin overlying vadose zone, and obtained results indistinguishable from previous models considering pure conduction with a uniform thermal conductivity. These studies shed light on limitations of the g-function solution commonly used to model the subsurface. One possibility for the insensitivity of the borehole heat transfer problem to the presence of a vadose zone is that the depth of the water table considered was only a small fraction of the borehole length. Another issue is that fluid flow for the considered problem was very small.

Therefore, we considered a much deeper water table, whose depth varied. These simulations were conducted with TOUGH only and remain to be coupled to Modelica, but the preliminary finding is that even with a thicker vadose zone, and significant liquid- and gas-phase flow, but no regional groundwater flow, the borehole heat transfer problem remains insensitive to fluid flow. The nature of the fluid flow varied considerably for the different cases considered, from natural convection cells when the water table was stable, to strong up and down flow when the water table depth varied. The magnitude of the fluid flow within the subsurface and out the surface also varied strongly among the cases, but the subsurface temperature distributions and heat transfer in and out of the borehole and ground surface did not.

Our tentative conclusion is that the extreme aspect ratio of the storage system (100+ m long and only 3-m wide), makes it strongly conduction dominated. All the simulations so far have been for axisymmetric representations of a single long borehole within a large borefield consisting of closely-spaced boreholes. The next step will be to consider different borehole/borefield geometries. The simplest extension will be to consider shorter, more widely spaced boreholes, which may be attractive because they could reduce drilling costs. Such systems can be examined with axisymmetric models. True 3D models are needed for the following stage, when regional groundwater flow will be considered. Here, the overall geometry of the borefield will also become important, with long and thin borefields, sited to fit into irregular or limited spaces, producing much different results than square borefields.

ACKNOWLEDGMENT

This material was based upon work supported by the U.S. Department of Energy, Office of Energy Efficiency and Renewable Energy (EERE), Geothermal Technologies Office, Low-Temperature Geothermal Program, under Award Number DE-AC02-05CH11231 with LBNL.

REFERENCES

Amili, P. and Yortsos, Y.C.: Stability of heat pipes in vapor-dominated systems, *Int. J. Heat and Mass Transfer*, 47, (2004), 1233-1246.

Akrouch, G.A., Sánchez, M, and Briaud, J.-L.: An experimental, analytical and numerical study on the thermal efficiency of energy piles in unsaturated soils, *Computers and Geotechnics*, 71, (2016), 207-220.

Başer, T. Dong, Y., Moradi, A.M., Lu, N., Smits, K., Ge, S., Tartakovsky, D. and McCartney, J.S.: Role of nonequilibrium water vapor diffusion in thermal energy storage systems in the vadose zone, *J. Geotech. Geoenviron. Eng*., 144(7), (2018), 04018038.

Catolico, N., Ge, S., and McCartney, J.S.: Numerical modeling of a soil-borehole thermal energy storage system, *Vadose Zone Journal*, doi:10.2136/jzj2015.05.0078, (2016).

Claesson, J. and Javed, S.: A Load-Aggregation Method to Calculate Extraction Temperatures of Borehole Heat Exchangers. *ASHRAE Transactions* 118(1), (2012), 530-539.

Dong, Y., McCartney, J.S., and Lu, N.: Critical review of thermal conductivity models for unsaturated soils, *Geotech. Geol. Eng*., 33, (2015), 207-221.

Hu, J., Doughty, C., Dobson, P., Nico, P., Wetter, M., Coupling Subsurface and Above-Surface Models for Design of Borefields and Geothermal District Heating and Cooling Systems, *Proceedings*, 45th Workshop on Geothermal Reservoir Engineering, Stanford University, Stanford, California, (2020).

Jung, Y., Pau, G., Finsterle, S., and Doughty, C.: TOUGH3 User's Guide, Version 1.0, *Report LBNL-2001093*, Lawrence Berkeley National Laboratory, Berkeley, Calif., (2018).

Moradi, A., Smits, K.M., Lu, N., and McCartney, J.S.: Heat transfer in unsaturated soil with application to borehole thermal energy storage, *Vadose Zone Journal*, doi:10.2136/vjz2016.03.0027, (2016)

NOAA, National Oceanic and Atmospheric Administration website: ncdc.noaa.gov/cdo-web/, Climate Data Online, Monthly Normals, accessed February 1, (2021).

Picard, D. and Helsen, L.: Advanced Hybrid Model for Borefield Heat Exchanger Performance Evaluation: An Implementation in Modelica, *Proceedings*, the 10th International Modelica Conference, p. 857-866. Lund, Sweden. (2014).

Pruess, K., Oldenburg, C., and Moridis, G.: TOUGH2 User's Guide, Version 2.1, *Report LBNL-43134*, Lawrence Berkeley National Laboratory, Berkeley, Calif., (2012).

van Genuchten, M.Th.: A closed form equation for predicting the hydraulic conductivity of unsaturated soils, *Soil Sci. Soc. Am. J*. 44, (1980), 892–898.

Wetter, M., Zuo, W., Nouidui, T.S., and Pang, X.: Modelica Buildings Library, *J. Building Performance Simulation*, **7**, (2014), 253–270.

Xu, T., Sonnenthal, E., Spycher, N., and Zheng, L.: TOUGHREACT V3.0-OMP Reference Manual: A Parallel Simulation Program for Non-Isothermal Multiphase Geochemical Reactive Transport, *Report LBNL-DRAFT*, Lawrence Berkeley National Laboratory, Berkeley, Calif., (2014).